Article

Not peer-reviewed version

How Acid Washing Nickel Foam Substrates Improves the Efficiency of the Alkaline Hydrogen Evolution Reaction

Thomas B Ferriday *, Suhas Nuggehalli Sampathkumar, Peter Hugh Middleton, Jan Van Herle, Mohan Lal Kolhe

Posted Date: 4 January 2023

doi: 10.20944/preprints202301.0055.v1

Keywords: acid washing; nickel foam; hydrogen evolution reaction; alkaline water electrolysis; electrode preparation

Article

How Acid Washing Nickel Foam Substrates Improves the Efficiency of the Alkaline Hydrogen Evolution Reaction

Thomas B. Ferriday[1,2]*, Suhas Nuggehalli Sampathkumar[2], Peter Hugh Middleton[1], Jan Van Herle[2] and Mohan Lal Kolhe[1]

[1] Department of Engineering Science, University of Agder, NO-4879 Grimstad, Norway
[2] Group of Energy Materials, Swiss Federal Institute of Technology, Lausanne (EPFL), 1951 Sion, Switzerland
* Correspondence: thomasbf@uia.no

Abstract: Nickel foam substrates are frequently utilised for renewable energy applications as porous 3D-substrates. Preparation of these substrates usually includes an acid washing step, however the degree to which this step affects the final electrochemical performance after spray coating a catalyst ink is unreported. Herein, we report the effect of acid washing through physicochemical and electrochemical characterisation. The electrochemical performance was determined by repeated measurements of catalyst-coated nickel foam substrates both with and without the initial step of acid washing. Acid washing increased current density by 17.9% for the acid treated, MoS_2-coated nickel foam electrode. This increment was affiliated with an electrochemically active surface area which increased by 87.1%, where Tafel analysis indicated that the acid treated, MoS_2-coated electrodes facilitates the initial water dissociation step of the hydrogen evolution reaction with greater ease. Similar effects were also discovered for acid treated PtIr(1:3)/C-coated nickel foam substrates, albeit with less pronounced effects. Stability was also improved where the degradation rate was reduced by 18.9% for the acid treated, MoS_2-coated electrodes. This proves the utility of acid washing nickel foam electrodes.

Keywords: acid washing; nickel foam; hydrogen evolution reaction; alkaline water electrolysis; electrode preparation

1. Introduction

The ongoing renewable energy transition includes new energy carriers such as hydrogen [1–4], where production through water electrolysis yields green hydrogen. Key to this process is the hydrogen evolution reaction (HER), which is one of the two half-cell reactions in water electrolysis [5]. The advent of the novel anion exchange membrane (AEM) [1–4] has caused a shift within water electrolysis creating a greater emphasis on alkaline water electrolysis utilising AEM technology. The alkaline HER is currently under profound scrutiny, as there is considerable difficulty in finding stable catalyst materials capable of replacing platinum group metals (PGMs) [5]. As such, methods of improving the performance of non-PGM catalyst materials is subject to ample R&D efforts.

Chief among such methods is acid washing, where the current trend in technologies related to both water electrolysis, batteries, and general electrochemistry for electrode preparations includes this step [6–19]. The utility of acid washing is great with respect to decreasing the influence of organic contaminants and reducing the surface oxide layer. The benefits include a notable reduction in series resistance, thus enabling greater performance and tenacity. However, there is great disparity in the manner in which this step is carried out, with respect to acid type and concentration.

There are reports utilising hydrochloric acid, sulphuric acid, perchloric acid, nitric acid [6–19] and likely several other options, where the concentration varies from weak dilute acids around 0.05 M [6,7] to undiluted acids [8–12] and everything in between [13–19]. The influence of acid washing has been characterised for use in batteries and supercapacitors [20], medical implants [21] and the alkaline

Preprints (www.preprints.org) | NOT PEER-REVIEWED | Posted: 4 January 2023 doi:10.20944/preprints202301.0055.v1

oxygen evolution reaction [22]. The implications of corrosion during hydrothermal processes for direct catalyst growth onto nickel foam support was investigated [23]. It was determined that the nickel foam may indeed supply nickel ions which may alter the catalyst composition, proving that catalytic influence of the support cannot be neglected during processes such as electrodeposition.

However, the effects of acid washing nickel foam supports for the alkaline hydrogen evolution reaction remain largely unreported. Hitherto unpublished work displays a notable improvement in both series resistance and charge transfer resistance in bare nickel foam substrates as alkaline HER electrodes from utilising both hydrochloric and sulphuric acid, where the latter outperformed the former [24]. A peak performance was achieved by acid washing with 0.50 M sulphuric acid, yielding a notable decline in series resistance []. It is highly common to apply a catalyst ink to a substrate through spray-coating, though degree to which the aforementioned benefits of acid washing persist after spray-coating is currently unknown, where the same applies to the lifetime of such benefits. Herein, we seek to fill this void in literature by testing multiple catalyst coated nickel foam substrates in an efficient three-electrode setup both with and without the initial step of acid washing.

2. Experimental

A three electrode setup was utilised, consisting of a nickel foam working electrode, a platinum wire counter electrode and an extended Luggin probe (agar salt bridge) connected with a Ag/AgCl reference electrode. The nickel foam electrode was pressed against a gold current collector to reduce ohmic resistance as shown in Figure 1. The small-scale setup with fixed distance between the three electrodes allowed for a high degree of reproducibility.

The use of ionic bridges (extended Luggin probes) was essential to allow the reference electrodes to fit into the half-cell shown in Figure 1. These ionic bridges were produced by mixing 22.37 g KCl (Sigma Aldrich) into 100 mL deionised water and heating until the boiling point was reached. From here, 1.5 g (1.5 wt.%) of Difco Agar (Fischer Scientific) was carefully added, thereby creating a 3.0 M KCl solution covered in Agar gel in liquid form. While the mixture was boiling, a tube attached to a syringe was employed to suck the solution into the tubing, thus filling the entire volume of both tubing and syringe. This was left overnight to settle, creating an ionic bridge ready for the insertion of Ag/AgCl (3.0 M KCl) reference electrodes the next day.

Deionised water and an appropriate quantity of potassium hydroxide (powder) for synthesis (Sigma Aldrich) were combined to create the 1.0 M KOH electrolyte, which was thoroughly hand-stirred to ensure a homogeneous concentration. The three-electrode setup was left to settle to establish steady state, by allowing the electrolyte to completely permeate all cavities of the nickel foam electrode.

The non-PGM inks were created by mixing 11 mg of MoS_2 powder (US Nano) with 1.5 mL deionised water, 0.5 mL isopropanol and 22 mg of Sustainion® XB-7 alkaline ionomer. The PGM ink was created by distributing 3 mg 10 wt.% PtIr(1:3)/C (fuelcellstore.com) in 1 mL deionised water, 1.0 mL isopropanol and 6 mg of Sustainion® XB-7 alkaline ionomer (DiOxide Materials). These dispersions were ultrasonicated for 15 minutes, where the resulting inks were spray-coated onto four 1 cm^2 nickel foam electrodes. These electrodes were attached to an aluminium plate heated to approximately 80°C. These four electrodes comprise two MoS_2 electrodes and two PtIr(1:3)/C electrodes, one acid-treated and one regular for both types of electrode. Several sets of electrodes were created to allow additional control experiments to be executed.

Preprints (www.preprints.org) | NOT PEER-REVIEWED | Posted: 4 January 2023 doi:10.20944/preprints202301.0055.v1

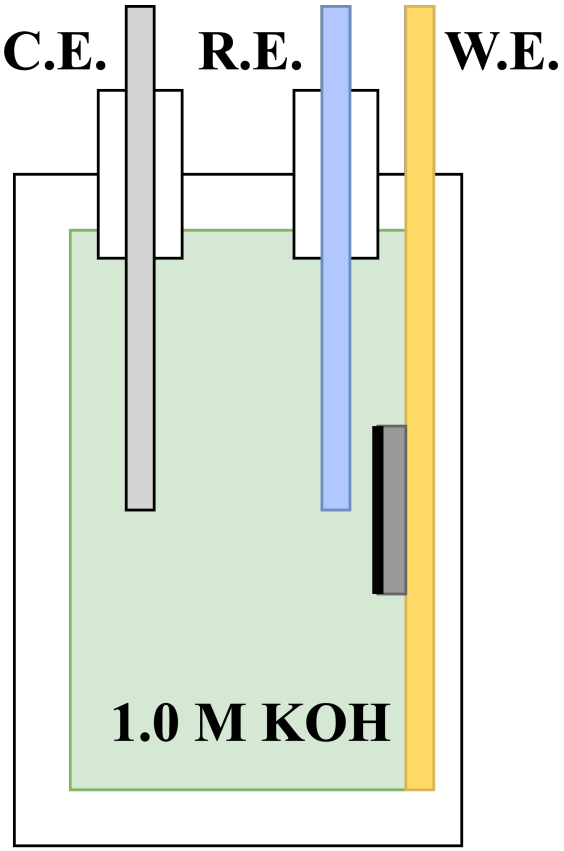

Figure 1. An efficient three electrode setup with a platinum wire counter electrode (C.E), an extended Luggin probe connected to a Ag/AgCl reference electrode (R.E) and a catalyst coated nickel foam working electrode (W.E) attached to a gold plate to decrease ohmic losses. All electrochemical characterisation was performed in 1.0M KOH at room temperature.

The electrochemical results were procured utilising an Iviumstat electrochemical workstation. Electrochemical impedance spectroscopy (EIS) spectra at open circuit were initially collected at the frequencies 10^5–10^{-1} Hz with a sinusoidal perturbation of 10 mV and 10 points per decade. This was followed by polarised EIS spectra at -50, -100, -150 and -200 mV relative to the hydrogen evolution reaction (HER). Linear sweep voltammetry (LSV) curves were subsequently recorded between 0.3 to -0.3 V_{RHE} at 10 mV s^{-1}, and repeated to guarantee repeatability. This data was utilised to determine Tafel slopes. The electrochemical double layer was determined through cyclic voltammetry (CV) between 0.346 to 0.446 V_{RHE} at scan speeds of 10 to 20 mV s^{-1} with 2 mV increments. To ensure stability, the initial scan at 10 mV s^{-1} was repeated until all scans were overlapping. Stable CV results were obtained once scans at the slowest rate (10 mV s^{-1}) were stable. Chronopotentiometry was performed at 10 mA cm^{-2} for 12 h in 1.0 M KOH at room temperature to ascertain stability. The degradation rates were determined based off the same starting point at -0.20 V_{RHE}. This sequence was repeated for all electrodes to improve the basis for comparative work, and multiple versions of each electrode type were tested to ensure stability and repeatability.

The surface morphology of the nickel foam electrodes was analysed in a Jeol JSM-7200F field emission scanning electron microscope (SEM). Multiple points were analysed to ensure a solid foundation for determining the atomic composition of the surface. X-ray diffraction (XRD) was performed with a Bruker D8 Advance where all Bragg Brentano measurements were made in reflection mode. The X-ray source was a Cu kα (1.5406 Å), operated at 40 kV, 40 mA (1600 W). The peaks were fitted utilising Fityk with a pseudo-voigt function utilising the Rietveld refinement method.

Preprints (www.preprints.org) | NOT PEER-REVIEWED | Posted: 4 January 2023 doi:10.20944/preprints202301.0055.v1

3. Results & discussion

3.1. Microstructural characterisation

The effect of acid washing was ascertained through scanning electron microscopy (SEM), energy dispersive X-ray spectroscopy (EDS) and X-ray diffraction (XRD). The effect of acid washing for increasingly potent concentrations of sulphuric acid is illustrated in Figure 2. Change in surface morphology is clear, where comparing the pristine reference nickel foam in Figure 2a to the surfaces in Figure 2b-2g. The degree of uniform corrosion increases together with the influence of pitting corrosion. The reference nickel foam in Figure 2a exhibits a clean, untainted surface, whereas the surface treated with 2.0 M H_2SO_4 bears little resemblance. The degree of uniform surface corrosion has decreased the influence of pitting corrosion due to its severity.

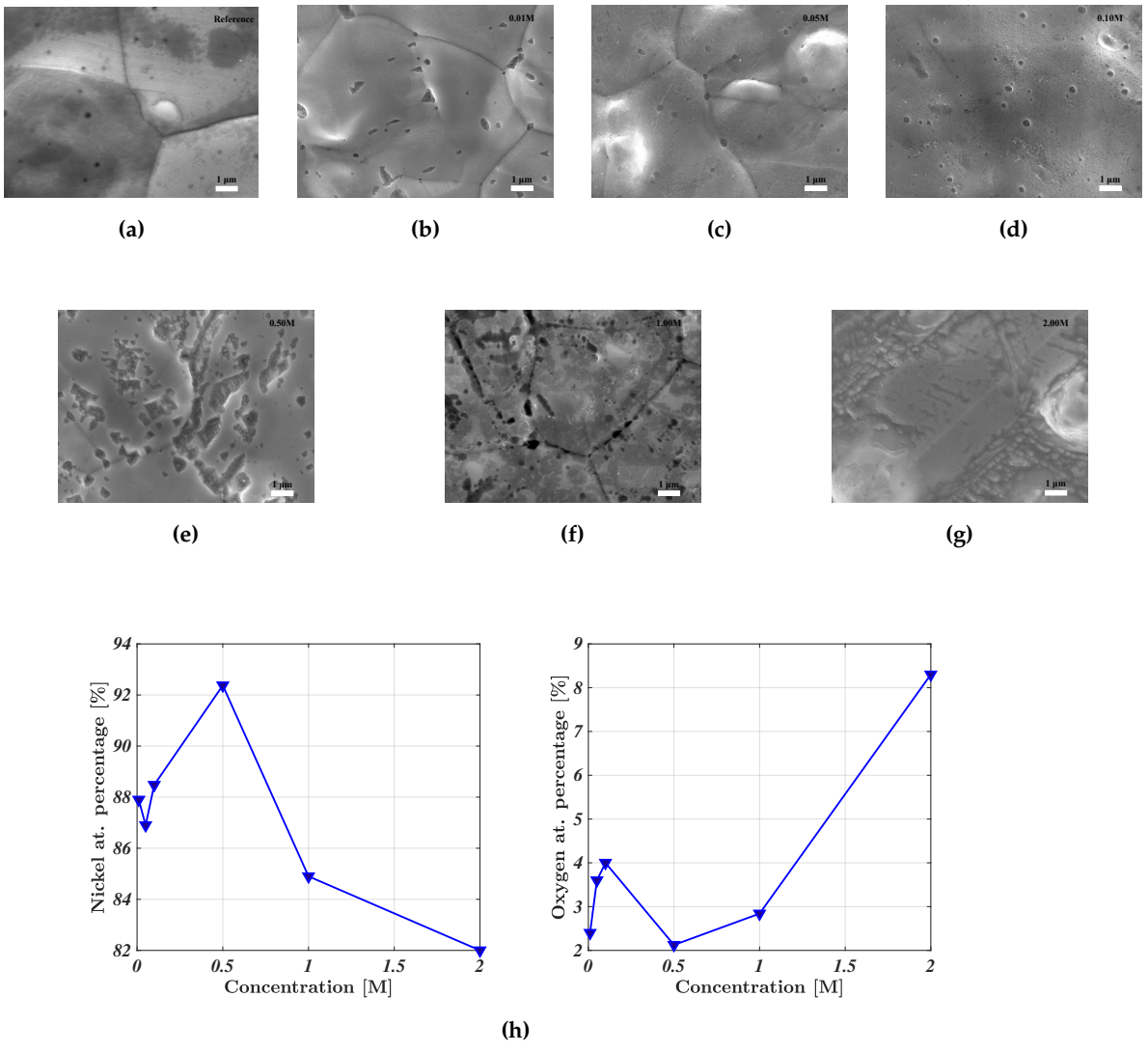

Figure 2. **(a)-(g)** SEM figures of the pristine H_2SO_4-treated nickel foam electrodes showing the gradual increase in surface roughness. **(h)** EDS-determined atomic surface concentration of nickel and oxygen.

EDS results indicate a nadir/peak in the atomic percentage of oxygen/nickel respectively for the nickel foam electrode treated with 0.50 M sulphuric acid. This affirms previous work showing a nadir for the EIS-determined series resistance for the same acid concentration. Greater acid concentrations resulted in greater/lower concentrations of oxygen/nickel as shown in Figure 2h, thus agreeing with previous electrochemical evidence indicating decreased influence of a surface oxide layer. For great

Preprints (www.preprints.org) | NOT PEER-REVIEWED | Posted: 4 January 2023 doi:10.20944/preprints202301.0055.v1

acid concentrations, the uniformity of the surface decreased simultaneously with a greater influence of oxygen. This is contradictory to the intention of acid washing, namely to reduced the effect of surface oxides. The electrodes were exposed to air during sample mounting for SEM/EDS analysis. Thus the increase in oxygen surface concentration after 0.50 M sulphuric acid may be related to an increased propensity to form an oxide layer once exposed to air after acid washing with great concentrations (>0.50 M H_2SO_4).

Shown in Figure 3a is the XRD spectra for select concentrations of the acid-treated nickel foam electrodes. The electrodes presented a singular cubic phase fm-3m, where the highlighted peaks are affiliated with the 111- and 200 facets of nickel foam at 44.61-44.69° and 51.96-52.07° respectively (JCPDS No. 87-0712) [25]. The minor variation in peak position (0.08°) for the 0.05 M sample originates most likely from height variations during sample mounting due to the porous nature of the nickel foam electrodes. The peaks were fitted allowing the extraction of the lattice parameters and d-spaces for the two peaks as shown in Fig.3b. Both the lattice parameter *a* and the d-spacing increases slightly with increasing acid concentration. The increase in lattice parameter *a* follows the same trend as the nickel at.% . The change in lattice parameter implies increasing lattice distortion with increasing acid concentration, where this would likely increase further as the acid concentration exceeds 0.50 M [26].

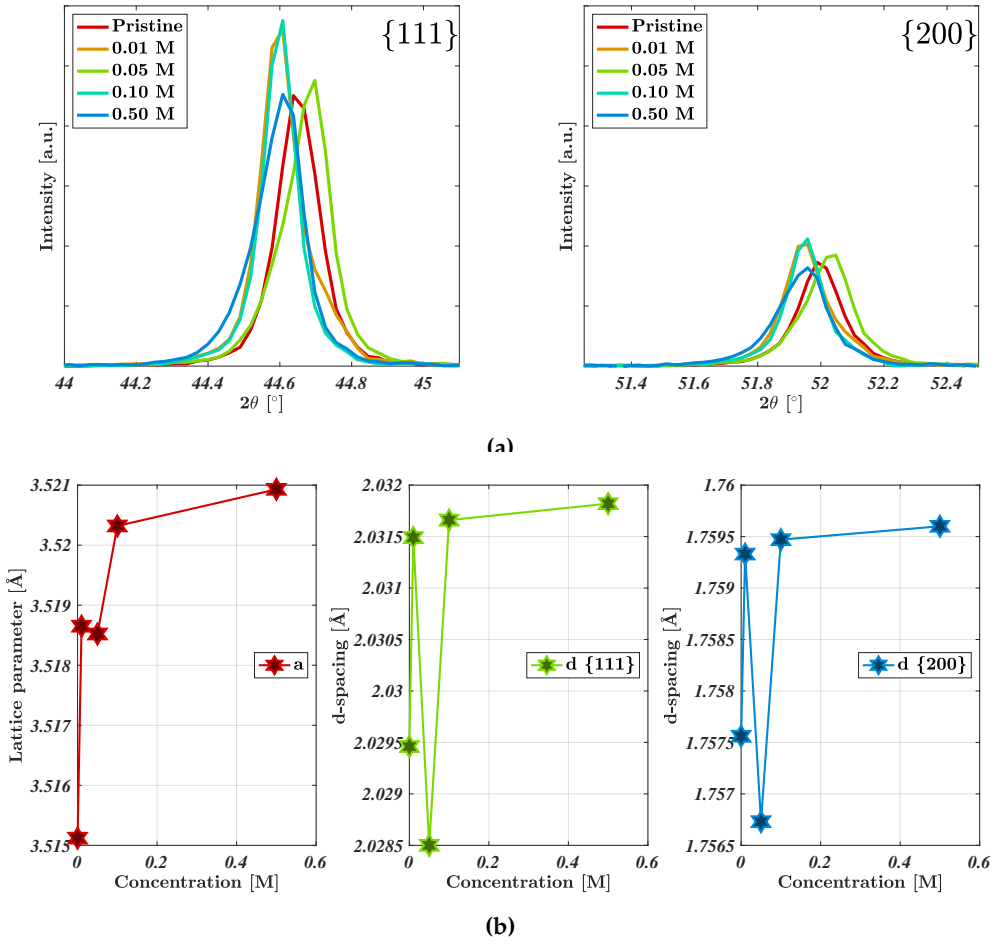

Figure 3. (**a**) XRD spectra of the acid-treated nickel foam electrodes, highlighted for the principal peaks related to the 111 and 200 facets respectively. (**b**) Lattice parameter and d-spacing extracted from the XRD data in (**a**).

Preprints (www.preprints.org) | NOT PEER-REVIEWED | Posted: 4 January 2023 doi:10.20944/preprints202301.0055.v1

3.2. Electrochemical Characterisation

The following section details the results from the electrochemical characterisation. These results were procured following the protocol detailed in the experimental section. The effect of spray-coating acid treated nickel foam electrodes was tested for two different types of catalyst ink, specifically non-PGM MoS_2 and PGM PtIr(1:3)/C. LSVs were recorded for the four types of electrodes between 0 to -0.3 V_{RHE} as shown in Figure 4a. The acid-treated MoS_2 and PtIr(1:3)/C electrodes outperform the untreated electrodes by 17.9% and 5.19% respectively. Predictably enough, the PGM electrode surpassed the performance of the non-PGM MoS_2-coated electrode. The rationale for this performance increment was dissected through determining the electrochemical double layer C_{dl} (Figure 4b), which scales linearly with the electrochemically active surface area (ECSA). Both the acid-treated, spray coated electrodes display fair improvement relative to the regular spray coated electrodes. However, the improvement was notably greater for the MoS_2-coated, acid treated electrode where the ECSA increased with 87.2%. The ECSA of the acid treated, PtIr(1:3)/C-coated electrode improved by 20.7%. Acid treatment with 0.50 M H_2SO_4 caused notable changes to the surface as shown in the SEM images in Figure 2, where this increased inhomogeneity was likely a great contributor to the augmented surface.

These are similar trends to that seen in the polarised EIS spectra in Figure 4c. The MoS_2-coated, acid treated electrode displays a fair improvement with respect to the charge transfer resistance, amounting to a 14.3% reduction. This displays that while the series resistance is similar, a performance increment is still achieved through reducing the charge transfer resistance. This adheres to established trends in unpublished research [24] displaying that while acid treatment reduced the series resistance, the decline in charge transfer resistance is greater. Both versions of the PtIr(1:3)/C coated electrodes display a similar total impedance spectra, though there was a slight change in capacitance which correlates with the 20.7% improvement in C_{dl}.

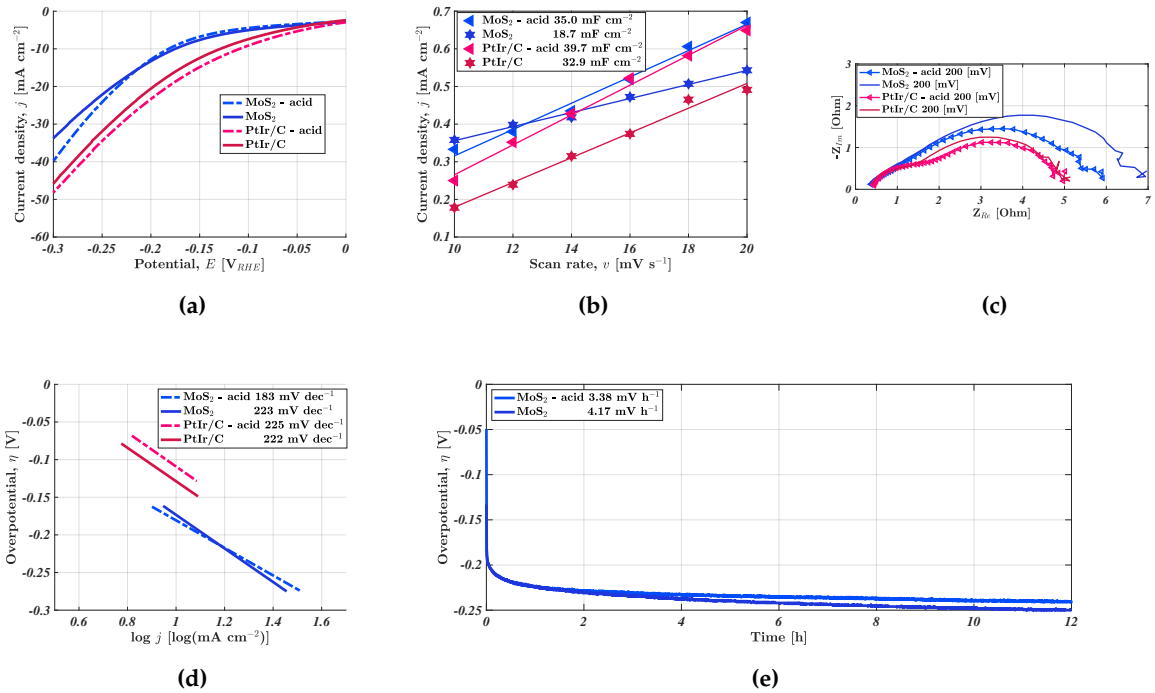

Figure 4. Electrochemical results detailing the effects of acid treatment upon the resulting performance in 1.0 M KOH at room temperature. (**a**) Linear sweep voltammetry, (**b**) the electrochemical double layer, (**c**) Nyquist plots at 200 mV overpotential relative the HER and (**d**) Tafel slopes. The stability at 10 mA cm^{-2} over 12 hours is shown in (**e**). All overpotentials are relative to the hydrogen evolution reaction.

 doi:10.20944/preprints202301.0055.v1

Tafel curves in Figure 4d indicate that the MoS_2-coated, acid treated electrode displays a reduction in Tafel slope, while the affiliated slopes of both versions of the PtIr(1:3)/C were largely similar. Moreover, the MoS_2-coated, untreated electrode displays a Tafel slope very similar to the PtIr(1:3)/C-coated electrodes. The reduction in Tafel slope for the MoS_2-coated, acid treated electrode indicates an improved pathway for hydrogen evolution. While both slopes indicate that the Volmer step (water dissociation) is rate limiting, the use of acid treatment would appear to improve the efficiency of this step. The stability of these improvements was tested by performing CP as shown in Figure 4e, where the degradation rate of the MoS_2-coated, acid treated electrode was lower than the untreated version of the non-PGM HER electrode. The 18.9% lower degradation rate (3.38 mV h^{-1}) shows the improvements induced by the acid treatment do not immediately abate during continuous operation. This indicates the possibility of greater longevity when including the initial acid washing step prior to catalyst coating.

4. Conclusions

This paper investigates how acid washing nickel foam substrates affects the performance and stability of the electrodes after they have been spray coated with a catalytic ink. The electrochemical performance of catalyst-coated nickel foam was evaluated for both acid-treated and untreated nickel foam for two types of catalytic ink. By employing MoS_2- or PtIr(1:3)/C-coated nickel foam as a hydrogen evolution reaction electrode in 1.0 M KOH, it was clear that the acid washing positively affected the performance of both types of HER-electrode. The LSV performance of the acid-treated, MoS_2- and PtIr(1:3)/C-coated electrodes increased by 17.9% and 5.19% respectively. This was correlated with an augmented ECSA as shown by CV and EIS spectra. A great ECSA improvement was noted for the MoS_2-coated electrode which increased by 87.2%. Tafel analysis indicates an improvement in the water dissociation step which likely contributed to the enhanced LSV performance. Stability also appeared to increase after acid washing, where the degradation rate was lowered by 18.9%. These results demonstrate the utility of acid washing substrates prior to the application of a catalyst layer.

Author Contributions: Conceptualisation, T.B.F. and S.N.S.; methodology, T.B.F. and S.N.S.; software, T.B.F.; validation, T.B.F. and S.N.S.; formal analysis, T.B.F. and S.N.S.; investigation, T.B.F.; resources, P.H.M., J.V.H., M.L.K.; data curation, T.B.F.; writing—original draft preparation, T.B.F.; writing—review and editing, T.B.F. and S.N.S.; visualisation, T.B.F.; supervision, P.H.M., J.V.H., M.L.K.; project administration, P.H.M., J.V.H., M.L.K.; funding acquisition, P.H.M., J.V.H., M.L.K. All authors have read and agreed to the published version of the manuscript.

Funding: This research received no external funding.

Conflicts of Interest: The authors declare no conflict of interest.

References

1. Ferriday, T.; Middleton, P. Alkaline fuel cell technology - A review. *International Journal of Hydrogen Energy* **2021**, *46*, 18489–510.
2. Ferriday, T.; Middleton, P. 4.07 - Alkaline Fuel Cells, Theory and Applications. In *Comprehensive Renewable Energy (Second Edition)*, Second ed.; Letcher, T., Ed.; Elsevier: Oxford, 2022; pp. 166–231.
3. Vincent, I.; Lee, E.C.; Kim, H.M. Comprehensive impedance investigation of low-cost anion exchange membrane electrolysis for large-scale hydrogen production. *Scientific Reports* **2021**, *11*, 1–12.
4. Varcoe, J.; Atanassov, P.; Dekel, D.; Herring, A.; Hickner, M.; Kohl, P.; Kucernak, A.; Mustain, W.; Nijmeijer, K.; Scott, K.; et al. Anion-exchange membranes in electrochemical energy systems. *Energy & environmental science* **2014**, *7*, 3135–91.
5. Ferriday, T.; Middleton, P.; Kolhe, M. Review of the Hydrogen Evolution Reaction—A Basic Approach. *Energies* **2021**, *14*, 8535.
6. Akhtar, N.; El-Safty, S.; Khairy, M.; El-Said, W. Fabrication of a highly selective nonenzymatic amperometric sensor for hydrogen peroxide based on nickel foam/cytochrome c modified electrode. *Sensors and Actuators B: Chemical* **2015**, *207*, 158–66.

7. Dong, S.; Ji, X.; Yu, M.; Xie, Y.; Zhang, D.; He, X. Direct synthesis of interconnected porous carbon nanosheet/nickel foam composite for high-performance supercapacitors by microwave-assisted heating. *Journal of Porous Materials* **2018**, *25*, 923–33.
8. Chaudhari, N.; Jin, H.; Kim, B.; Lee, K. Nanostructured materials on 3D nickel foam as electrocatalysts for water splitting. *Nanoscale* **2017**, *9*, 12231–47.
9. Zhang, C.; Du, X.; Wang, Y.; Han, X.; Zhang, X. $NiSe_2$@ Ni_xS_y nanorod on nickel foam as efficient bifunctional electrocatalyst for overall water splitting. *International Journal of Hydrogen Energy* **2021**, *46*, 34713–26.
10. Lu, L.; Hou, D.; Fang, Y.; Huang, Y.; Ren, Z. Nickel based catalysts for highly efficient H2 evolution from wastewater in microbial electrolysis cells. *Electrochimica Acta* **2016**, *206*, 381–7.
11. Ji, B.; Zhao, W.; Duan, J.; Fu, L.; Ma, L.; Yang, Z. Immobilized Ag_3PO_4/GO on 3D nickel foam and its photocatalytic degradation of norfloxacin antibiotic under visible light. *RSC advances* **2020**, *10*, 4427–35.
12. Pierozynski, B.; Mikolajczyk, T.; Kowalski, I. Hydrogen evolution at catalytically-modified nickel foam in alkaline solution. *Journal of Power Sources* **2014**, *271*, 231–8.
13. He, Z.; Sun, J.; Wei, J.; Wang, Q.; Huang, C.; Chen, J.; Song, S. Effect of silver or copper middle layer on the performance of palladium modified nickel foam electrodes in the 2-chlorobiphenyl dechlorination. *Journal of Hazardous Materials* **2013**, *250-251*, 181–89.
14. Shih, Y.J.; Wu, Z.L.; Huang, Y.H.; Huang, C.P. Electrochemical nitrate reduction as affected by the crystal morphology and facet of copper nanoparticles supported on nickel foam electrodes (Cu/Ni). *Chemical Engineering Journal* **2020**, *383*, 123157.
15. Sarawutanukul, S.; Phattharasupakun, N.; Wutthiprom, J.; Sawangphruk, M. 3D CVD graphene oxide on Ni foam towards hydrogen evolution reaction in acid electrolytes at different concentrations. *ECS Transactions* **2018**, *85*, 49.
16. Lu, X.; Pan, J.; Lovell, E.; Tan, T.; Ng, Y.; Amal, R. A sea-change: manganese doped nickel/nickel oxide electrocatalysts for hydrogen generation from seawater. *Energy & Environmental Science* **2018**, *11*, 1898–1910.
17. Li, X.; Zhang, Z.; Xiang, Q.; Chen, R.; Wu, D.; Li, G.; Wang, L. A three-dimensional flower-like NiCo-layered double hydroxide grown on nickel foam with an MXene coating for enhanced oxygen evolution reaction electrocatalysis. *RSC advances* **2021**, *11*, 12392–97.
18. Bai, J.; Sun, Q.; Wang, Z.; Zhao, C. Electrodeposition of cobalt nickel hydroxide composite as a high-efficiency catalyst for hydrogen evolution reactions. *Journal of The Electrochemical Society* **2017**, *164*, H587.
19. Dastafkan, K.; Li, Y.; Zeng, Y.; Han, L.; Zhao, C. Enhanced surface wettability and innate activity of an iron borate catalyst for efficient oxygen evolution and gas bubble detachment. *Journal of Materials Chemistry A* **2019**, *7*, 15252–61.
20. Ansari, S.; Parveen, N.; Al-Othoum, M.; Ansari, M. Effect of washing on the electrochemical performance of a three-dimensional current collector for energy storage applications. *Nanomaterials* **2021**, *11*, 1596.
21. Hung, K.Y.; Lin, Y.C.; Feng, H.P. The Effects of Acid Etching on the Nanomorphological Surface Characteristics and Activation Energy of Titanium Medical Materials. *Materials* **2017**, *10*, 1164.
22. Kim, M.; Kim, J.; Qin, L.; Mathew, S.; Han, Y.; Li, O.L. Gas-Liquid Interfacial Plasma engineering under dilute nitric acid to improve hydrophilicity and OER performance of nickel foam. *Progress in Natural Science: Materials International* **2022**, *32*, 608–616.
23. Bu, X.; Wei, R.; Cai, Z.; Quan, Q.; Zhang, H.; Wang, W.; Li, F.; Yip, S.; Meng, Y.; Chan, K.; et al. More than physical support: The effect of nickel foam corrosion on electrocatalytic performance. *Applied Surface Science* **2021**, *538*, 147977.
24. T.B. Ferriday, S.N. Sampathkumar, P.H. Middleton, J. Van Herle. Investigation of Wet-Preparation Methods Of Nickel Foam For Alkaline Water Electrolysis. *Journal of Physics* **2023**.
25. Long, L.; Yao, Y.; Yan, M.; Wang, H.; Zhang, G.; Kong, M.; Yang, L.; Liao, X.; Yin, G.; Huang, Z. Ni_3S_2@polypyrrole composite supported on nickel foam with improved rate capability and cycling durability for asymmetric supercapacitor device applications. *Journal of Materials Science* **2017**, *52*, 3642–3656.
26. Niu, J.; Liu, X.; Xia, K.; Xu, L.; Xu, Y.; Fang, X.; Lu, W. Effect of electrodeposition parameters on the morphology of three-dimensional porous copper foams. *Int. J. Electrochem. Sci* **2015**, *10*, 7331–7340.